

Pairing evidence of 8CB molecules adsorbed on MoS₂: Influence of 2D commensurability on the intralamellar structure

E. Lacaze¹, M. Alba², M. Goldmann^{3,4}, J.P. Michel¹ and F. Rieutord⁵

¹ *Groupe de Physique des Solides, Universités Paris 7 et 6, UMR-CNRS 75-88, 2 place Jussieu, 75251 Paris CEDEX, France*

² *DRECAM/SPEC, bat 772, CE-Saclay, 91191 Gif sur Yvette CEDEX, France*

³ *LURE, Bat 209D, Université Paris Sud, 91405 Orsay CEDEX, France*

⁴ *GRPB, Université Paris 5, 45 rue des Saints Pères, Paris CEDEX 6, France*

⁵ *CEA-Grenoble, DRFMC/SI3M/MCI, 17 rue des Martyrs, 38054 Grenoble CEDEX 9, France*

By combining X-ray diffraction studies under grazing incidence (GIXD) and Scanning Tunneling Microscopy (STM) measurements, we have precisely determined the structure of 8CB molecules adsorbed on MoS₂, under the thick organic film. The commensurability of the adsorbed network and the intracell structure have been determined, revealing a complex structure characterized by a non-equivalence of adjacent lamellae with pair associations of molecules in one lamella over two. We have interpreted such a result by a simple model of a single lamella. This pair association in one lamella over two appears as a direct evidence of the connection between the commensurabilities in the two directions. The value of the molecule-substrate potential corrugations is particularly high, indicating that the dipolar momentum of 8CB molecules could play a fundamental role in the molecule-substrate interactions.

PACS 61.10.-i, 68.35.Bs, 61.30, 68.35.Md

I. INTRODUCTION

Since the last decade, various interfaces between organic films and crystals have been described as well ordered in 2D, whereas the organic bulk is obviously liquid or liquid crystal¹. This is even true on chemically inert crystals, such as graphite or MoS₂ where molecules are only physisorbed, as probed by a number of Scanning Tunneling Microscopy (STM) measurements²⁻⁶. These interfaces are interesting in particular for two reasons. First, they can be studied very precisely at ambient temperature, as presented in the present article, which has led to the possibility of connecting the microscopic structure of the first adsorbed molecules to the relevant surface interactions; second, the structure is studied under the organic film which can lead in a second step to studies of the propagation of interfacial ordering into the organic bulk. In case of liquid crystal phases (8CB bulk is smectic at ambient temperature), this phenomenon is called anchoring⁷. In the case of physisorbed rare gas atoms or simple molecules on the same substrates, isotropic structures are formed, so that equilibrium structures can be exactly calculated⁸. They are described as commensurate or incommensurate with respect to the substrate. These structures can be generally described with one or two molecules in the crystallographic cell, such that the structure is completely determined by its commensurability. Organic molecules are more complex and exact calculations are already extremely more difficult to perform. However their study in the adsorbed configuration can be considered as a first step towards even more complex adsorbed molecules as for example biological molecules.

On graphite or MoS₂ substrates, organic molecules are usually organized in lamellae which can be straight or regularly kinked^{9,10}. Until now, the molecule-substrate interactions have been considered in some numerical calculations¹¹ or through a phenomenological Landau de Gennes-type model¹⁰. This mean-field model describes the monolayer structure as lamellae, which periodicity is imposed by the substrate, ignoring the intra-lamella structure. Structures are described as commensurate (straight lamellae) or incommensurate (kinked lamellae) with respect to the substrate, depending mainly on the ratio between the

substrate-molecule and molecule-molecule interactions and on the mismatch between the natural periodicity of the lamellae and the one imposed by the substrate. This model allows a global interpretation of the STM results and leads to a commensurate description of various structures which are naively expected to be incommensurate on such substrates since the molecules-substrate interactions are expected to be weak, in particular weaker than on metallic substrates^{12–14}. In order to confirm such results, we have studied a straight lamellae interface, which is “a priori” commensurate, as probed by STM³: 4-8-alkyl-4'-cyanobiphenyl (8CB) molecules adsorbed on molybdenum disulphide (MoS₂) substrate. STM images of 8CB on MoS₂^{3,10} reveal that the molecules are flat on the substrate, organized in straight lamellae, with a head to tail geometry. By combining two techniques, STM and X-ray diffraction at grazing incidence (GIXD), we have verified the commensurability of the interfacial structure and we have also precisely determined the intralamellar structure, allowing to go beyond the phenomenological model and to propose a study of the relationship between microscopic structures and interface interactions in physisorbed molecules.

The combination of STM and GIXD experiments appeared particularly useful for the determination of such adsorbed structures. Single monolayers only are often studied in case of adsorbed organic molecules^{14–16}. They can be observed by combining LEED and Auger experiments. In the case of an interface between a substrate and a thick organic film, these LEED and AUGER measurements are unoperating due to the presence of the bulk and mainly two techniques remain available, STM and GIXD. However it is difficult to image simultaneously the substrate and the adsorbed molecules by STM, especially in case of a semi-conducting substrate as MoS₂ (by contrast to graphite as substrate¹⁵). Another limitation of STM techniques is due to drift phenomena of the piezoelectric materials used for scanning the sample surface, preventing a precise estimation of absolute distance values. Finally, as the contrast in STM images is not perfectly understood, the precise molecular structure is difficult to infer from the images. On the other hand the Bragg peaks coming from the monolayer and from the substrate structures can be simultaneously obtained from GIXD experiments. This allows a precise determination of the relative orientation of the

two structures as well as of the lattice constants and of the molecule localizations which can be extracted with a precision as good as 0.5 Å. The major disadvantage of this latter technique remains the complexity of the experiment mainly due to the small amount of matter contained in physisorbed organic monolayers which imposes the use of synchrotron sources. This complexity justifies that up to now mainly STM experiments have been performed on such interfaces. However the refinement of X-ray data can be strongly simplified if one introduces constraints on the molecule position parameters. These constraints can be obtained from STM images, leading then to a fruitful combination of the two techniques. To our knowledge the only physisorbed organic film studied by combined STM and GIXD has been the 10CB/graphite system, showing metastable commensurate structure, coexisting with the a priori more stable incommensurate one¹⁷. In the first part of this article, we describe the experimental details; in a second part, the X-Ray diffraction results; in a third part, we analyse the peak intensities through a model of the molecules localization in the monolayer crystallographic cell. Finally in a fourth part, we discuss the energetic balance between molecule-molecule and molecule substrate interactions by developing an unilamellar model of the monolayer structure.

II. EXPERIMENTAL

The 8CB film has been prepared by melting the organic material on top of a freshly cleaved MoS₂ substrate, at 80°C. The 8CB is a BDH product used without any purification. MoS₂ natural single crystal comes from Australia (Queensland) through the Wards' company. This lamellar compound can be easily cleaved, giving a surface parallel to the basal planes. The surface plane is composed of sulphur atoms organized with an hexagonal symmetry (3.16 Å as cell parameter), with less than 0.02° mosaicity, as checked by X-Ray diffraction. Grazing incidence X-Ray diffraction experiments have been performed on beam-lines BM32 at ESRF and D41 at LURE. The incident beam (8 keV) reaches the interface through the 8CB bulk at an incidence of 0.5°, comparable to the MoS₂ critical

angle and larger than the 8CB bulk one. The diffracted intensity is scanned parallel to the plane by a linear detector covering an angle of 13° (PSD) perpendicular to the surface at LURE-D41 and a solid state detector at ESRF-BM32. The in-plane resolution is of the order of 1 mrad. The beam size width is about $500\text{ }\mu\text{m}$ and its intensity is monitored by a diode. The STM and GIXD experiments have been performed on many different samples. Always reproducible results have been obtained, but only the most intense Bragg peaks of the monolayer structure were observed at LURE-D41.

III. RESULTS

31 in-plane diffraction peaks (Table I, fig. 1) of the adsorbed molecules have been measured. They can be indexed in a (4x8) superstructure position, indicating that the monolayer structure is indeed commensurate with the MoS_2 lattice. However such a unit cell contains only one lamella, and a close inspection of the STM images indicates that the number of non equivalent lamellae is 4. Considering this constraint, the basic unit corresponds to a (4x32) superstructure and each peak has been indexed in this (4x32) superstructure (fig. 1). The low index Bragg peaks of such a superstructure can not be observed since they are very close to the direct beam. An example of diffraction peak, (4,-48), is presented on the figure 2. The rocking curve (fig. 2a) indicates that the in-plane mosaicity (0.02°) mimics the substrate one, showing that the adsorbed monolayer is constituted of well-ordered single crystallized domains. The observed radial scan width (fig.2b) is limited by the experimental resolution, revealing a correlation length at least larger than $1000\text{ }\text{\AA}$.

The experimental intensities measured on a given sample (BM32 experiment) are indicated on Table 1. They have been obtained by a gaussian adjustment to the peak shapes. The reciprocal space have been explored along the twelve high symmetry directions and four main commensurate positions have been unambiguously assigned to a nul intensity after careful investigations. Since the θ -range is rather small ($\Delta\theta\leq 13^\circ$), we neglected any

geometrical correction. We used these intensity values to perform a refinement of the molecular structure: we start with an eight-molecule cell, built in order to form lamellae parallel to the MoS₂ [100] direction, with a head to tail geometry. The cell parameters are fixed to the (4x32) MoS₂ superstructure. Calculated intensities are adjusted to the measured ones with a least square criterium. Molecules are considered as flat on the substrate, therefore only 2D calculations are performed. They are divided in two rigid parts: the alkyl chain in trans configuration and the cyanobiphenyl part also flat on the substrate. The degrees of freedom of the model are the length of the alkyl chain and of the cyanobiphenyl group (considered as equal for all molecules), the angles between the alkyl chain and the cyanobiphenyl group (with an equal value for the molecules of same lamella), the location and the overall rotation of molecules. Considering the STM observations, and in order to limit the number of parameters, we divide the crystallographic cell in two blocks of four molecules, which can be translated one from each other, the value of the displacement being an adjustable parameter.

We consider two other fit parameters, anisotropic Debye-Waller terms and the monolayer 3-fold degeneracy. Indeed, due to the hexagonal symmetry of the MoS₂, three different directions (at $\pm 60^\circ$) are equivalent for the adsorbed 2D crystal. They can coexist on the sample, and their relative weight must be adjusted. Note that since the commensurabilities along the two high symmetry directions of the MoS₂ substrate are multiples from each other, Bragg peaks originating from two coexisting domains can be superimposed.

The best result ($\chi^2 = 3.19$) is presented on the figure 3a. The corresponding calculated Bragg peaks intensities, compared to the measured ones, are presented on the table I. The alkyl chain length is 0.866 nm, the cyanobiphenyl length 0.901 nm and the angles between them are 34.5° for one lamella and 35.2° for the other one. The displacement between the two four molecules blocks has been obtained as half the cell parameter. The crystallographic cell is then a "centered" c(4x32) superstructure of the MoS₂. Considering that the 8CB cell is eight times longer along the k direction than along the h direction, an STM images can be normalized in order to avoid the deformations connected to the drift of the piezoelectric

materials and superimposed to the fit solution. Such a comparison, presented on the figure 3b, shows that the refinement result is in very good agreement with the STM observations, in particular the different orientations and locations of the eight molecules in the cell.

IV. DISCUSSION

A. Molecular conformation

We have allowed independent values for the angles between the alkyl chain and the cyanobiphenyl group of the molecules of two successive lamellae. Values very close from each other are finally obtained, also similar to the one calculated for an isolated flat molecule, 35.5° . This indicates that the adsorbed 8CB molecules on MoS₂ are essentially not distorted, which is coherent with the numerical calculation of 8CB molecules adsorbed on graphite¹¹, but differs from the recent observations on organic molecules covalently bonded onto Ag(111)¹⁸. The obtained lengths of the alkyl chain and of the cyanobiphenyl group are close (about 10% larger) to the ones estimated for an isolated flat molecule in a completely trans conformation. This confirms that the adsorbed molecules are lying flat on the substrate, with the alkyl chain, completely elongated, in all trans conformation. This indicates that, in their isotropic phase, the molecules are mobile enough to find their 2D-crystallized equilibrium conformation, with only very few gauche defects¹⁴. Due to the number of measured Bragg peaks, we could not consider the possibility of rotation of the phenyl groups, but the good agreement between the measured and calculated Bragg intensities indicates that, if such a rotation occurs, it remains small. The observed flat conformation of the molecules is clearly related to a strong molecule-substrate interaction.

B. Unilamellar model

The observation of a pair association in one lamella over two is probably the most spectacular result of these X-ray measurements (fig. 3). We underline that such a non-equivalence

of two successive lamellae, with the presence of pair-associations in one lamella and equidistant molecules in the neighboring one, is a particularly robust result which appears almost systematically in the fit solutions. Avoiding pair association lead to very high χ^2 values. It demonstrates that, whatever organized in a commensurate network, the adsorbed molecules do not lie on identical adsorption sites. The origin of such a feature is probably connected to the microscopic interactions between molecules as well as between molecules and the substrate, which can not be described in a mean field model. In order to check this assumption, we have built a simple model for a single lamella. We consider a commensurate model, with two dipoles which can be displaced anywhere in the cell, with an antiferroelectric alignment. The knowledge of the 8CB characteristics (dipole ($D = 4.9$ D)^{19,11}, polarizability ($\alpha = (40 \cdot 10^{-30} \cdot 4\pi\epsilon_o) \text{ m}^3$)²⁰, ionization potential ($I = 8.7\text{eV}$, derived from the diphenyl one by analogy with the hydrocarbons case)²¹ allows the calculation of the energy per molecule as a function of the distance, r , between the molecule and its first neighbours²²:

$$\begin{aligned}
E &= E_D + E_{VdW} + E_S \\
&= -\frac{D^2}{4\pi\epsilon_o} \left(\frac{1}{r^3} + \frac{1}{(4a-r)^3} \right) \\
&\quad - \frac{3\alpha^2 I}{(4(4\pi\epsilon_o)^2)} \left(\frac{1}{r^6} + \frac{1}{(4a-r)^6} \right) \\
&\quad + C \left(\frac{1}{r^{12}} + \frac{1}{(4a-r)^{12}} \right) \\
&\quad + E_o - B \cos 2\pi \left(\frac{2a-r}{2a} \right)
\end{aligned} \tag{1}$$

with r in \AA and the energy in J. E_D is the term of dipolar interactions between adjacent molecules. E_{VdW} is the term of Van der Waals interactions between adjacent molecules which includes the dispersion forces as well as a steric repulsion where C is a phenomenological value as usual. The attractive dispersion interactions appear to be about three to four times larger than the attractive dipolar ones, by varying the distances between molecules from 4.3 to 6.32 \AA , as already pointed out by Tildesley et al.¹¹ [note1]. E_S is the molecule-substrate potential which is described by a constant term E_o for the adsorption energy, and an oscillating term, the potential corrugations, which period is fixed to the MoS₂ cell

parameter $a = 3.16\text{\AA}$.

Plotting the energy as a function of r leads to two types of configuration, depending on the substrate corrugations parameter, B (fig. 4). If B is strong, one minimum minimorum appears, corresponding to a location of the molecules in the substrate potential wells (fig. 4c). The intermolecular distance is then $r_1 = 2a = 6.32\text{\AA}$. If B is weak, two r values give equal energy minima and pair associations are formed (fig. 4a). The molecules are located out of the potential wells and the intermolecular distance is mainly imposed by the balance between attractive dipolar, dispersion interactions and steric repulsion. One can then calculate C by neglecting $B \cos 2\pi(2a-r/2a)$: we have determined through our X-ray refinement a pair intermolecular distance of 4.3\AA (r_2) which leads to $C = 5.088 \cdot 10^{-12} \text{J } \text{\AA}^{12}$. A first order transition between the two configurations occurs for a critical value B_c ($B_c = 7.45 \cdot 10^{-20} \text{J}$) which can be calculated by equating the two energy minima at r_1 and r_2 (fig. 4b):

$$B_c = \frac{1}{1 - \cos 2\pi \left(\frac{2a - r_2}{2a} \right)} \star \left[-\frac{D^2}{4\pi\epsilon_o} \left(\frac{2}{r_1^3} - \frac{1}{r_2^3} - \frac{1}{(4a - r_2)^3} \right) - \frac{3\alpha^2 I}{(4(4\pi\epsilon_o)^2)} \left(\frac{2}{r_1^6} - \frac{1}{r_2^6} - \frac{1}{(4a - r_2)^6} \right) + C \left(\frac{2}{r_1^{12}} - \frac{1}{r_2^{12}} - \frac{1}{(4a - r_2)^{12}} \right) \right] \quad (2)$$

The observation of the two kinds of solutions on the same sample, one lamella with pair associations, adjacent to one lamella with equidistant molecules, indicates a variation of the substrate corrugation parameter from $B \leq B_c$ to $B \geq B_c$ between two successive lamellae. This has to be correlated to the refinement results which indicates an average difference in molecular orientations of around 10° for two neighboring lamellae. This directly demonstrates the anisotropic nature of the molecule-substrate corrugations which depend on the orientation of the molecule with respect to the substrate crystallographic directions. We can

also conclude that the calculation of B_c gives a minimum value for the substrate corrugation which indeed stabilizes the observed configuration with equidistant molecules: $7.45 \cdot 10^{-20}$ J per molecule (i.e. $17 k_B T$). We checked that this value is independent of the precise form of the repulsion function and remains identical for different type of repulsive functions (for example varying as C/r^9 or C/r^{15}).

C. commensurability of the lamellae

The explanation for the observed alternate solution needs to go beyond the unilamellar model described above. It can be justified by considering the 2D structure associated to a single type of lamella. If one considers a $c(4 \times 32)$ superstructure composed by equidistant molecules only, a limited number of possibilities exists due to the commensurability of the molecules location. It appears then that, in each case, the cyanobiphenyl groups of adjacent lamellae would be located directly in front of each other. Such a $c(4 \times 32)$ superstructure suffers then from strong steric incompatibilities and a $c(4 \times 34)$ superstructure appears to be the smallest superstructure which does not exhibit such a steric repulsion. However in a $c(4 \times 34)$ superstructure the mismatch between the lamellae period imposed by the substrate and the natural lamellae period would jump from 2.5% to 9%. Such a lack of compacity would become unfavorable for the attractive part of the interactions between adjacent lamellae: indeed 11CB molecules on MoS_2 with a 10% similar mismatch relax by creating kinks leading to an incommensurate structure perpendicularly to the lamellae¹⁰. Alternating two intralamellar structures favours the attractive interactions without inducing steric repulsion due to different locations of the cyanobiphenyl groups of adjacent lamellae. On the other hand, a 2D structure composed of pair associations only would correspond to a completely incommensurate structure within the lamellae. Consequently, in our model the postulated commensurability is in fact imposed by the interaction between adjacent lamellae. The observed alternating structure appears as a compromise which allows to preserve the commensurability in both directions, within the lamellae and between the lamellae. The energy

gain of the perpendicular commensurability is balanced by the presence of pair associations, a priori less favorable, one lamella over two. It shows how the commensurabilities of these structures in both directions are strongly correlated and cannot be described through a phenomenological model which ignores the intralamellar structures. It justifies to perform now similar X-ray studies on 9CB and 11CB on MoS₂, since our result suggests that 9CB and 11CB lamellae on MoS₂ which are kinked^{23,10}, should present a single type of lamellae with a commensurate intra-lamellar structure.

D. Molecule-substrate interaction

The obtained value of the substrate corrugations is high, $7.45 \cdot 10^{-20} \text{ J}$ ($17 \text{ k}_B \text{ T}$) and such, consistent with the observation of a commensurate structure at ambient temperature and to its thermal stability [note2]. Very few data exist for evaluating it more precisely, especially in case of MoS₂. Best of available studies deal with rare gas atoms on graphite. In case of xenon atoms on graphite, the substrate corrugation has been estimated at about $2.78 \cdot 10^{-21} \text{ J}$ ^{24,25}, 27 times smaller than our estimated value of 8CB on MoS₂.

Substrate-atoms interactions are only of the Van der Waals type in the Xe/graphite system. Calculating the homogeneous Van der Waals part of the molecule-substrate interactions through a continuous model²⁶, one obtains a value 15 times smaller for the Xe/graphite system^{27,28} than for the 8CB/MoS₂ one^{29,30} instead of the 27 times for the substrate potential corrugations ($(0.25 \alpha_{Xe})/D^3 \text{ J}$ compare to $(0.38 \alpha_{8CB})/D^3 \text{ J}$, with D the distance in Å between the Xe or the 8CB and the substrate and α the polarizability)^{20,22}. However the 8CB/MoS₂-Xe/graphite corrugations ratio is expected to be smaller than the 8CB/MoS₂-Xe/graphite homogeneous potentials ratio, due to the large and anisotropic size of the 8CB which should average and such diminish the substrate corrugations compare to the Xe atoms. In the way to explain the calculated increasing, one can assume that the previous lamellar model overestimate the corrugation parameter, B. Calculating the dipolar interaction for two 8CB molecules, as they are located in the structure, one obtains only a 1.06% increase with

respect to the model result. However, Van der Waals interactions between the molecules may have been overestimated due to the far location of the more polarizable cyanobiphenyl groups in the antiferroelectric alignment. Another possibility is that the 8CB/MoS₂ corrugation potential is not only related to pure Van der Waals interactions. This is supported by the presence of a strong dipolar momentum, 4.9D, located on the cyanobiphenyl group in 8CB molecules possibly inducing special molecule-substrate interactions, apart the pure Van der Waals ones. Dipole-induced dipole interactions have a negligible influence compare to Van der Waals ones, as shown by continuous calculations ($8.10^{-20}/D^3$ J compare to $2.43 \cdot 10^{-18}/D^3$ J). However one should consider that MoS₂ is composed of two types of atoms, which differences in polarizabilities could play a role. Numerical calculations could test such an hypothesis. Clearly such an effect should be absent on graphite, as shown in the study of polar molecules as CH₂Cl₂ adsorbed on graphite³¹. This result on MoS₂ suggests that the location of the cyanobiphenyl groups with respect to this substrate should play a predominant role as it is generally assumed that the alkyl chains determine the structure on the graphite substrate.

V. CONCLUSION

We have precisely determined, through a combination of scanning tunneling microscopy and grazing incidence X-rays diffraction, the 2D network of 8CB molecules adsorbed on MoS₂ which anchor along the [100] MoS₂ direction. The crystallographic cell has been determined, as well as the intracell fine structure. The X-ray diffraction spectra refinement lead a molecular structure very close to the STM images. Introduction of constraints in the refinement method allows a reduction of the a priori large number of fit parameters, connected to the size of the molecules and to the number of molecules in the unit cell. The constraints being directly defined by the STM results, this demonstrates how the combination between the two techniques (STM and GIXD) is fruitful. In the reverse way, the X-ray results evidence the fine structures within the lamellae, which are not straightforward in the

STM images.

The structure appears to be commensurate, perpendicularly to the lamellae as predicted by a phenomenological model¹⁰, but moreover within the lamellae. The 8CB crystallographic cell is a centered $c(4 \times 32)$ MoS₂ superstructure

The determination of the crystallographic parameters is clearly not sufficient to describe correctly the adsorbed network. The description of the intracell structure evidences complex intralamellar structures that we have interpreted through an unilamellar model of the microscopic interactions. Pair associations in one lamella over two correspond to lamellae with molecules out of the molecule-substrate potential wells adjacent to lamellae with molecules inside the wells. This alternating series reflect the connection between the commensurabilities along and perpendicularly to the lamellae. The critical value of the molecule-substrate potential corrugations which impose the observed commensurate lamellae has been calculated to be $7.45 \cdot 10^{-20}$ J per molecule. This particularly high value with respect to the Xe/graphite system could be connected to the presence of a high dipolar momentum in the 8CB molecules. The anisotropy of these corrugations is already demonstrated, directly connected to the orientation of the molecules with respect to the substrate crystallographic directions. Numerical simulations as well as similar measurements on slightly different systems could now be very usefully compared to such a study, in order to go towards the complete understanding of the complex interactions substrate-organic molecules. This could allow, in the future, of directly forecasting adsorbed structures of molecules, at least in case of physisorption.

Note1:

This observation justifies the occurrence of two different structures for only slightly different molecules on the same substrate: a "single layer" one for 8CB on MoS₂, which lamellae are characterized by an antiferroelectric alignment, a priori favorable for dipolar interactions; a "double layer" one for 10CB on MoS₂³², which lamellae are characterized by a ferroelectric alignment, unfavorable for dipolar interactions⁶. The relative lost of dipolar energy is even smaller for larger molecules (10CB compare to 8CB) and could be partly

compensated by a win in Van der Waals interaction connected to the proximity of the more polarizable cyanobiphenyl groups in the second structure. So the win in molecule-substrate interactions necessary for imposing a "double layer" structure can be only small and indeed correlated to some odd-even effect due to the position of the end of the alkyl chain on the underlying substrate, as recently proposed⁶. This remark also justifies the observation that in 10CB/graphite case the two types of structure have been evidenced, also through the association of STM and GIXD experiments¹⁷.

Note2:

The 8CB adsorbed layer Bragg peaks starts to disappear at 120°C only, whereas the 8CB bulk already starts to evaporate around 100°C.

- ¹ O. Marchenko and J. Cousty, Phys. Rev. Lett. **84**, 5363 (2000).
- ² J. Foster and J. Frommer, Nature **9**, 542 (1988).
- ³ M. Hara *et al.*, Nature **344**, 228 (1990).
- ⁴ J. Rabe, S. Buchholz, and L. Askadskaya, Physica Scripta Volume T **49**, 200 (1993).
- ⁵ K. Walzer and M. Hietschold, J. Vac. Sci. Technol. B **14**, 1461 (1996).
- ⁶ S. Taki, T. Kadotani, and S. Kai, Journal of the Physical Society of Japan **68**, 1286 (1999).
- ⁷ B. Jérôme, Rep. Prog. Phys. **54**, 91 (1991).
- ⁸ J. Villain and M. Gordon, Surf. Sci. **125**, 1 (1983).
- ⁹ Y. Iwakabe *et al.*, Japanese Journal of Applied Physics, Part 2 [Letters] **29**, L2243 (1990).
- ¹⁰ E. Lacaze, P. Barois, and R. Lacaze, J. Phys. I France **7**, 1645 (1997).
- ¹¹ D. Cleaver and D. Tildesley, Molecular Physics **81**, 781 (1994).

- ¹² A. Hoshino, S. Isoda, H. Kurata, and K. T., Journal of Applied Physics **76**, 4113 (1994).
- ¹³ S. Forrest and Y. Zhang, Phys. Rev. B **49**, 11297 (1994).
- ¹⁴ A. Soukopp *et al.*, Journal of the Physical Society of Japan **58**, 13882 (1998).
- ¹⁵ K. Walzer and M. Sternberg, M. Hietschold, Surf. Sci. **415**, 376 (1998).
- ¹⁶ H. Meyerheim and T. Gloege, Phys. Stat. Sol. (a) **173**, 175 (1999).
- ¹⁷ P. Dai *et al.*, Phys. Rev. B **47**, 7401 (1993).
- ¹⁸ H. Meyerheim *et al.*, Surface Review and Letters **6**, 883 (1999).
- ¹⁹ K. Gueu, E. Megnassan, and A. Proutierre, Mol. Cryst. Liq. Cryst. **132**, 303 (1986).
- ²⁰ M. Mitra, Phase Transitions **37**, 131 (1992).
- ²¹ F. Gutmann and L. Lyons, *Organic Semiconductors* (John Wiley and Sons, Inc., New York-London-Sidney, 1967).
- ²² J. Israelachvili, *Intermolecular and surface forces* (Harcourt Brace Jovanovitch, New York, 1991).
- ²³ Y. Iwakabe *et al.*, Japanese Journal of Applied Physics, Part 2 [Letters] **30**, 2542 (1991).
- ²⁴ W. A. Steele, Surf. Sci. **36**, 317 (1973).
- ²⁵ C. de Bauvais, Ph.D. thesis, Université Paris VII, 1986.
- ²⁶ J. Israelachvili, Q. Rev. Biophys. **6**, 341 (1974).
- ²⁷ E. Taft and H. Philipp, Phys. Rev. A **138**, 197 (1965).
- ²⁸ S. Ergun, in *Chemistry and Physics of carbon*, edited by M. Dekker (P.L. Walker Jr, New York, 1968), p. 48.
- ²⁹ B. Evans and P. Young, Proc. Roy. Soc. A **284**, 402 (1965).
- ³⁰ W. Liang, J. Phys. C **4**, L378 (1971).

³¹ A. Bah, Ph.D. thesis, Université Henri Poincaré de Nancy I, 1994.

³² Y. Iwakabe *et al.*, Japanese Journal of Applied Physics, Part 2 [Letters] **31**, L1771 (1992).

Bragg peak	I_m/I_o	I_c/I_o
(0,8,0)	0.16	0.12
(1,-8,0)	0.2	0.2
(0,14,0)	0	0
(2,-10,0)	0	0
(2,0,0)	1	1
(2,-16,0)	0.69	0.83
(0,-16,0)	0.81	0.85
(0,16,0)	0.81	0.85
(2,-24,0)	0.03	0.05
(3,-16,0)	0.02	0.12
(2,16,0)	0.06	0.05
(4,-16,0)	0.04	0.13
(3,8,0]	0.04	0.04
(3,-32,0)	0.09	0.07
(4,-24,0)	0.03	0.07
(3,-40,0)	0.03	0.05
(5,0,0)	0.01	0.01
(2,32,0)	0.20	0.14
(4,-48,0)	0.31	0.28
(4,16,0)	0.42	0.41
(6,-32,0)	0.49	0.61
(6,-16,0)	0.28	0.29

(0,48,0)	0.08	0.09
(6,0,0)	0.01	0
(6,-48,0)	0.60	0.60
(-7,0,0]	0	0
(2,48,0)	0.04	0.04
(6,16,0)	0	0
(8,-16,0)	0.03	0.03
(5,40,0)	0.02	0.02
(5,48,0)	0.02	0.02

TABLE I. 8CB Bragg peaks intensities normalized to the (2,0,0) peak: I_m/I_o measured intensities, I_c/I_o calculated intensities.

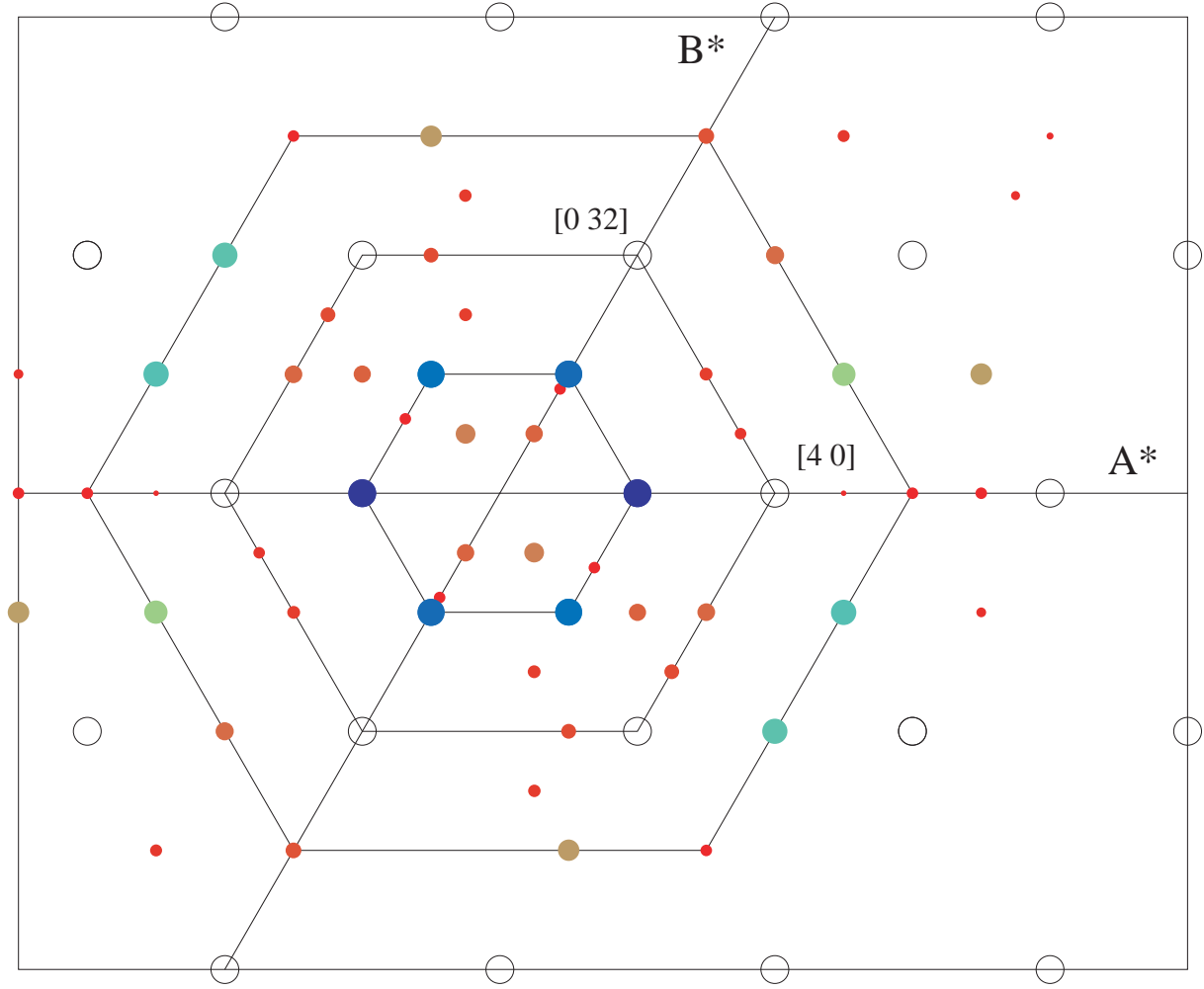


FIG. 1. Reciprocal space map of the 8CB/MoS₂ network. Open circles correspond to the MoS₂ bragg peaks and full ones to the 8CB ones which are indexed in the (4×32) superstructure of MoS₂. The intensities are qualitatively represented by the size of the circles.

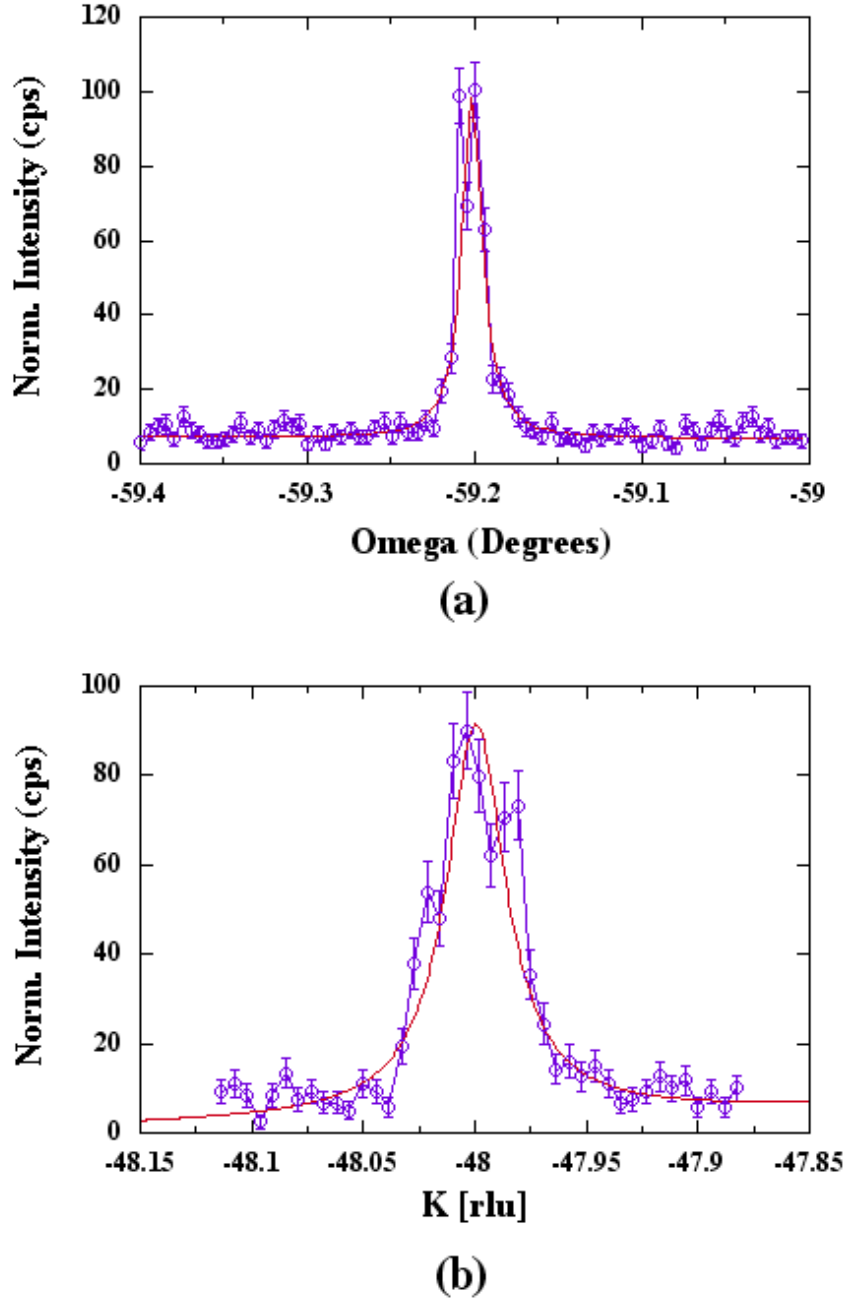
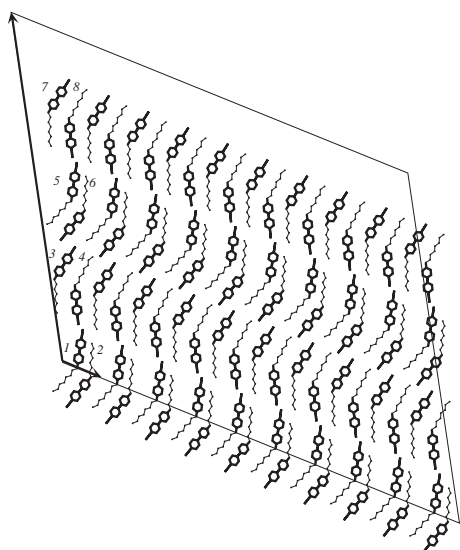
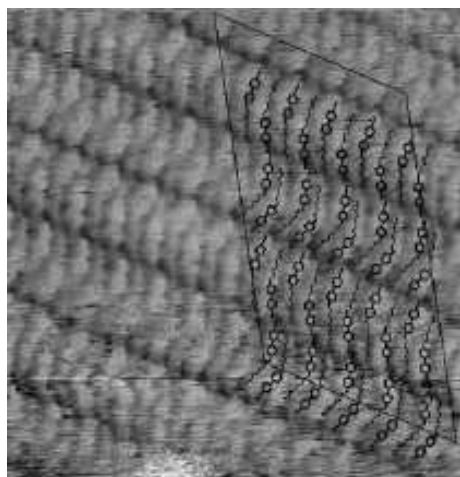


FIG. 2. a) rocking curve of the (4,-48,0) bragg peaks which indicates a mosaicity of 0.02° (the intensity, in count per second, is normalized to the incident beam intensity). b) radial curve of the (4,-48,0) bragg peaks which corresponds to a correlation length at least larger than 1000\AA .



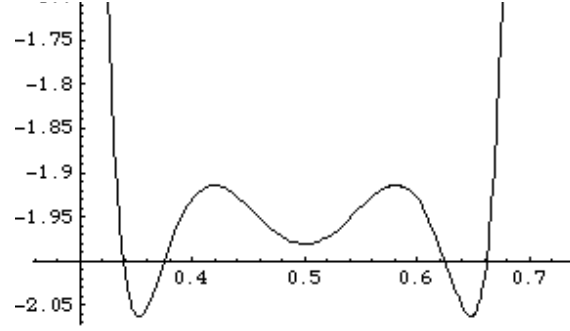
(a)



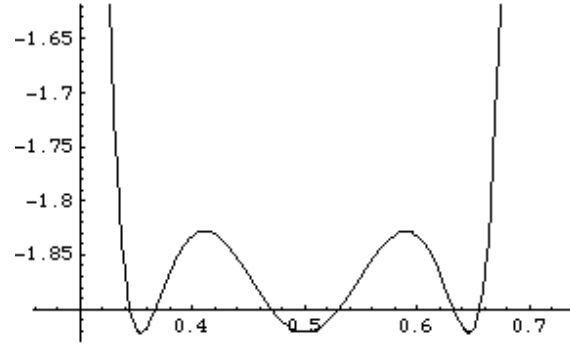
(b)

FIG. 3. a) result of the refinement of the X-ray data with the eight molecules of the crystallographic cell (the weights of the three possible orientations are 0.42 along the $[100]$, 0.21 along the $[010]$ and 0.37 along the $[1-10]$; the Debye-Waller coefficients are 0 along the $[100]$ and 0.02 along the $[010]$). Pair associations are formed between the molecules $1/2$ and $5/6$. b) comparison between the refinement and the STM image, rescaled.

$B = 7 \cdot 10^{-20} \text{ J}$



$B = 7.45 \cdot 10^{-20} \text{ J}$



$B = 8 \cdot 10^{-20} \text{ J}$

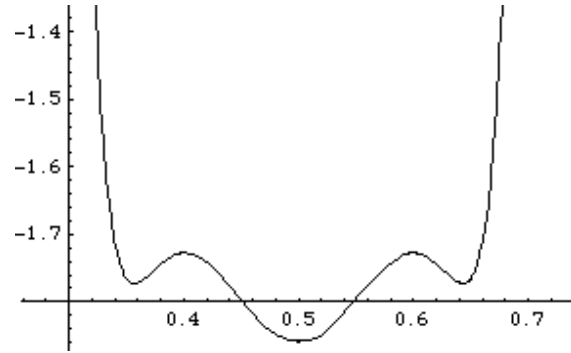


FIG. 4. energy (over B) of an 8CB molecule adsorbed on MoS₂ surface, versus r (Å) for various values of the corrugation potential, B: $B = 7 \cdot 10^{-20} \text{ J}$, $7.45 \cdot 10^{-20} \text{ J}$ and $8 \cdot 10^{-20} \text{ J}$.